Evidence of a significant rotational non-LTE effect in the CO2 4.3 μm PFS-MEX limb spectra

Alexander A. Kutepov, Ladislav Rezac, Artem G. Feofilov

Atmos. Meas. Tech., 10, 265–271, 2017
www.atmos-meas-tech.net/10/265/2017/
doi:10.5194/amt-10-265-2017

Atmospheric Measurement Techniques
Open Access
EGU

Evidence of a significant rotational non-LTE effect in the CO_2 4.3 µm PFS-MEX limb spectra

Alexander A. Kutepov[1,2], **Ladislav Rezac**[3], **and Artem G. Feofilov**[4]

[1]Space Weather Laboratory, NASA Goddard Space Flight Center, Greenbelt, MD, USA
[2]Physics Department, The Catholic University of America, Washington, D.C., USA
[3]Department of Planets and Comets, Max-Planck-Institut für Sonnensystemforschung, Justus-von-Liebig-Weg 3, 37077 Göttingen, Germany
[4]Laboratoire de Météorologie Dynamique, IPSL/CNRS, UMR8539, Ecole Polytechnique, Paris, France

Correspondence to: Alexander A. Kutepov (kutepov@cua.edu)

Received: 30 May 2016 – Published in Atmos. Meas. Tech. Discuss.: 27 June 2016
Revised: 17 November 2016 – Accepted: 9 December 2016 – Published: 24 January 2017

Abstract. Since January 2004, the planetary Fourier spectrometer (PFS) on board the Mars Express satellite has been recording near-infrared limb spectra of high quality up to the tangent altitudes $\approx$150 km, with potential information on density and thermal structure of the upper Martian atmosphere. We present first results of our modeling of the PFS short wavelength channel (SWC) daytime limb spectra for the altitude region above 90 km. We applied a ro-vibrational non-LTE model based on the stellar astrophysics technique of accelerated lambda iteration (ALI) to solve the multi-species and multi-level CO_2 problem in the Martian atmosphere. We show that the long-standing discrepancy between observed and calculated spectra in the cores and wings of 4.3 µm region is explained by the non-thermal rotational distribution of molecules in the upper vibrational states 10011 and 10012 of the CO_2 main isotope second hot (SH) bands above 90 km altitude. The redistribution of SH band intensities from band branch cores into their wings is caused (a) by intensive production of the CO_2 molecules in rotational states with $j > 30$ due to the absorption of solar radiation in optically thin wings of 2.7 µm bands and (b) by a short radiative lifetime of excited molecules, which is insufficient at altitudes above 90 km for collisions to maintain rotation of excited molecules thermalized. Implications for developing operational algorithms for massive processing of PFS and other instrument limb observations are discussed.

1 Introduction

For more than 6 Martian years the Planetary Fourier Spectrometer (PFS) on board the Mars Express satellite (Formisano et al., 2005) has been measuring the near-infrared radiances in both nadir and limb geometries. For the study of Martian middle and upper (60–130 km) atmosphere, limb measurements of the CO_2 4.3 µm emission are of particular interest as the source of information on density and thermal structure of this layer. These measurements are achieved by the PFS' short wavelength channel (SWC) [1.25–5 µm] with the spectral resolution allowing the unambiguous identification of many of the CO_2 emission bands. Details on the instrument description, its calibration and in-flight performance can be found in Formisano et al. (2005), Giuranna et al. (2005), and Formisano et al. (2006).

The strong daytime CO_2 4.3 µm emissions measured by PFS SWC are formed in the non-local thermodynamic equilibrium (non-LTE), which requires detailed accounting for the variety of processes influencing the ro-vibrational populations. The excitation of the $CO_2(\nu_3)$ vibrations is facilitated by absorption of solar radiation in the range of 1–2.7 µm by the CO_2 molecules. This excitation is followed by the cascade radiative one-quantum 4.3 µm transitions. In addition, the collisional quenching of molecular vibrations (V-T processes) and the inter- and intra-molecular exchange of vibrational energy (V-V processes) also strongly influence the populations.

A number of studies (López-Valverde et al., 2005; Formisano et al., 2006; López-Valverde et al., 2011a, b) (hereafter "previous studies") were undertaken in recent years aimed at interpretation of the PFS SWC limb spectra. These studies consider only vibrational non-LTE in CO_2 assuming molecular rotations completely thermalized (rotational LTE) and reiterate main features of daytime 4.3 µm CO_2 emission formation in the upper atmosphere, which is dominated by the second hot (SH) and third hot (TH) bands of the main CO_2 isotopologue (hereafter 626). Despite the good general understanding of how the absorption of solar radiation and subsequent redistribution of vibrational energy generate the hot CO_2 band emissions, significant features present in the measured PFS spectra remain unexplained. Specifically, the majority of the daytime limb radiance measurements above approximately 90 km exhibit substantially stronger emissions than predicted by the non-LTE models in the spectral ranges 2290–2305 and 2345–2355 cm^{-1} relative to the maxima of radiation at 2317 and 2335 cm^{-1}, respectively (López-Valverde et al., 2011b). An approach to explain this feature used in the previous studies was to treat the collisional rate coefficients as free parameters. However, the desired result was not reached, and it was speculated that remaining discrepancies might be due to contributions of some unidentified weak CO_2 4.3 µm bands not yet present in the HITRAN/HITEMP and GEISA spectroscopic databases. This issue remains unresolved until now. It prevents the scientific community from applying suitable retrieval algorithms for obtaining parameters of the Martian middle atmosphere from the PFS SWC limb spectra around 4.3 µm.

In this paper we address this long-standing discrepancy and provide its clear physical explanation.

2 Modeling the 4.3 µm emissions

2.1 The ALI-ARMS code

In this paper the CO_2 non-LTE populations and limb spectra are calculated using the ALI-ARMS (for Accelerated Lambda Iterations for Atmospheric Radiation and Molecular Spectra) non-LTE code package (Kutepov et al., 1998; Gusev and Kutepov, 2003; Feofilov and Kutepov, 2012). ALI-ARMS utilizes the accelerated lambda iteration (ALI) technique developed in stellar astrophysics (Werner, 1986, 1978; Rybicki and Hummer, 1991; Pauldrach et al., 1994, 2001; Pauldrach, 2003; Hubeny and Lanz, 2003) for calculating the non-LTE populations of a very large number of atomic and ionic levels in optically thick atmospheres. ALI has became a standard technique for spectrum formation calculations and for the computation of the non-LTE model stellar atmospheres. The ALI-ARMS code has been successfully applied to the diagnostics of a number of space infrared Earth's and Martian observations, both spectrally resolved (Kaufmann et al., 2002, 2003; Maguire et al., 2002; Gusev et al., 2006) and broadband signals (Kutepov et al., 2006; Feofilov et al., 2009, 2012; Rezac et al., 2015), as well as to study the infrared radiative cooling/heating in planetary atmospheres (Hartogh et al., 2005; Kutepov et al., 2007; Feofilov and Kutepov, 2012).

2.2 Rotational LTE and non-LTE

In order to establish a nominal result for a pure vibrational non-LTE model (complete rotational LTE is assumed) as used in previous studies, we run ALI-ARMS for our extended reference CO_2 model for a dust-free atmospheric model retrieved from the Mars Climate Database (hereafter MCD)[1], which matches the observation conditions. This reference model accounts for 150 vibrational levels of five CO_2 isotopologues and about 40 000 lines in calculating the non-LTE populations. The radiative transfer and solar absorption terms are calculated for all the 376 bands present in the task. We apply the same collisional rate coefficients for the lower vibrational levels as those used in previous studies. However, a different scaling of these basic rates for higher vibrational levels is performed based on the first-order perturbation theory as suggested by Shved et al. (1998).

Once the CO_2 populations are known we simulate the limb spectra in the range 2200–2400 cm^{-1} for different tangent altitudes both accounting for and not accounting for the overlapping and compare them to the PFS observations. In our model we include in total 60 bands of the five isotopologues that contribute to the CO_2 4.3 µm limb emission.

A random sample of the PFS measured spectrum is shown as a black curve in Fig. 1. This and other spectra have been kindly provided for this study by the PFS PI M. Giuranna. The shown spectrum is an average of 27 single scans taken for the following conditions: $L_s = 254$, latitude $= -67°$, local time = 18:00, and solar zenith angle (SZA) $= 69°$, and tangent height of 115 km. As we already noted the effect addressed here is present in the majority of daytime spectra. Therefore, no special criteria in latitude/longitude or local time were applied to select these particular spectra for comparison with calculations here. The turquoise curve in Fig. 1 presents the spectrum for our nominal run (these and other simulated spectra in this figure were obtained for SZA $= 69°$). We show here the synthetic radiance for tangent height of 120 km since for a given input atmospheric model it provides better agreement with measured spectrum at 115 km.[2] Comparison in Fig. 1 of simulated and measured signals obviously confirms the general conclusion of previ-

[1] http://www-mars.lmd.jussieu.fr/mars/access.html

[2] The mismatch of emission absolute values between measured and simulated spectra for the tangent altitude of 115 km (see also orange curve in Fig. 1, discussed below) may be attributed both to the mismatch of input model and to the simplifying assumptions applied in this and previous studies, namely, the missing field-of-view averaging.

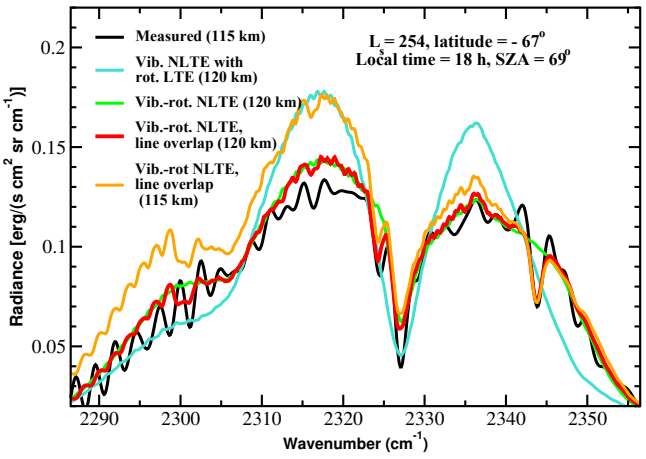

Figure 1. Comparison of measured (black) and simulated PFS SWC spectra. The observed spectrum is an average of 27 single scans taken for the following conditions: $L_s = 254$, latitude $= -67°$, local time = 18:00, SZA = 69°, and tangent height of 115 km. The 1σ random uncertainties for this measured spectrum are shown. The simulated spectra are shown for tangent height of 120 km including only vibrational non-LTE in CO_2 (turquoise), with vibrational–rotational non-LTE (green), and with vibrational–rotational non-LTE plus line overlapping along the line of sight (red). The spectra shown in orange color are calculated with the same assumptions as for red, but for tangent height 115 km as a demonstration (see text for detailed description).

ous studies: above the altitude of 90 km, no matter the location and local time, taking into account all known weak bands of CO_2 does not improve the mismatch with the observed radiance in the "shoulders" (2290–2305 and 2345–2355 cm^{-1}) relative to the maximum at 2317 and 2335 cm^{-1}.

The problem of "incorrect" radiance distribution between cores and wings of molecular bands is not a new one and has been theoretically investigated in a series of papers by Kutepov et al. (1985), Ogibalov and Kutepov (1989), and Kutepov et al. (1991) for CO_2 bands for atmospheric conditions of Mars and Venus, and for CO bands by Kutepov et al. (1997) for the Earth's atmosphere. In these studies it has been shown that in the Martian atmosphere the Boltzmann rotational distribution for CO_2 molecules in the ν_3-vibrationally excited states breaks down for altitudes above 80 km. At these altitudes the lifetime $\tau = 1/A$ of these vibrational levels, where $A \sim 200\,s^{-1}$ is the Einstein coefficient for the spontaneous 4.3 µm transitions, is not long enough for collisions to keep the rotation of excited molecules thermalized. Therefore, the need for complete vibrational–rotational non-LTE consideration had been identified already at that time.

In this study we relax the assumption of rotational LTE for two vibrational levels 10011 and 10012 (HITRAN notation) of main CO_2 isotope 626. These levels are strongly pumped by the absorption of solar radiation at 2.7 µm and give origin to the two strong SH bands, which dominate the 4.3 µm limb emissions (Gilli et al., 2009; López-Valverde et al., 2011a) of the Martian middle and upper atmosphere discussed here. We accounted for rotational sublevels up to $j = 102$ for each of these vibrational levels. The state-to-state rate coefficients describing rotational relaxation of vibrationally excited CO_2 were calculated as described by Kutepov et al. (1985), who applied the model of Preston and Pack (1977) and Pack (1979) based on infinite-order sudden (IOS) approximation results. The total rotational relaxation rate used in these calculations was estimated as $k_{rot}(T) = 2\pi k(T/p)\Delta\nu_L(T_o)(T/T_o)^{0.7}$, where $\Delta\nu_L$ is the Lorentz line width. The validity of this approach is discussed in detail for linear and nonlinear molecules by Hartmann et al. (2008). For our model we used mean Lorentz width $\Delta\nu_L$ of CO_2 rotational–vibrational lines from HITRAN12 (Rothman et al., 2013). Accounting for temperature dependence of these widths, $k_{rot} \approx 3 \times 10^{-10}\,cm^3\,s^{-1}$ for $T = 200$ K.

3 Results and discussion

3.1 Importance of rotational non-LTE

The green curve in Fig. 1 shows the spectrum calculated accounting for the rotational non-LTE at vibrational levels 10011 and 10012 of main CO_2 isotope. One may see that this spectrum shows the redistribution of the radiances from SH band branch cores into their wings and, as a result, reproduces the measured signal shape significantly better than calculations based on the assumption of rotational LTE (turquoise curve).

The reason for this alteration lies in the production of excited 626 molecules in vibrational states 10011 and 10012 due to the absorption of the 2.7 µm radiation in the altitude region of 80–140 km. In Fig. 2 (left panel) we show these production rates, normalized over the rotational quantum number j, for state 10011 at an altitude of 120 km for SZA = 69° (red), which corresponds to simulated spectra presented in Fig. 1. Additionally, the same pumping rates at 100 km for SZA = 60 and 80° (green and blue, respectively) are shown for comparison. Similar production rates were also obtained for level 10012. In general the molecules in level 10011 are most efficiently generated at the altitude of 120 km in rotational states with $j = 25$–40 (30–50 for altitude of 100 km). The low production for $j < 30$ is caused by a strong absorption of solar radiance in the cores of the 2.7 µm band branches in the upper atmosphere, which, however, remain transparent in the branch wings. At the altitudes above 90 km the collisions are not able to completely restore the Boltzmann rotational distribution of molecules in the vibrational states 10011 and 10012, and the latter takes the form shown in the right panel of Fig. 2. Compared to the Boltzmann distribution (red with circles), rotational non-LTE curve (red) demonstrates enhanced tail for $j > 30$, which reflects inten-

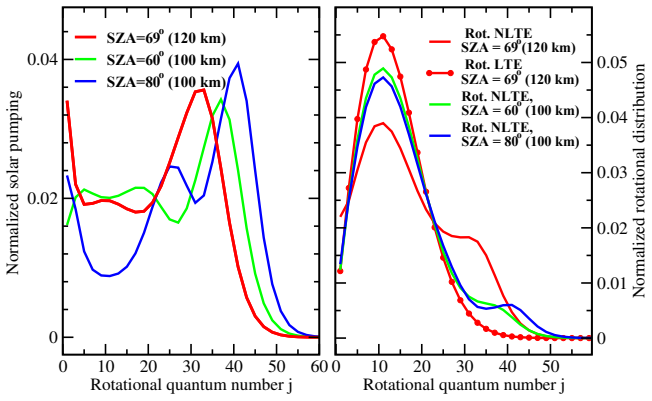

Figure 2. Left – normalized distribution of radiative pumping at level 10011 of $^{12}C^{16}O_2$ due to the absorption of the 2.7 µm solar radiation for altitudes of 100 and 120 km. Right – normalized rotational distribution at level 10011 of $^{12}C^{16}O_2$ for altitudes of 100 and 120 km.

sive radiative pumping of these levels shown in the left panel. The same is also true for two other curves (green and blue) shown in this panel for altitude 100 km. The latter demonstrate obvious dependence of the rotational LTE distortion on the SZA in agreement with corresponding production rate variation shown in the right panel of this figure.

3.2 Importance of line overlapping along the limb LOS

The rotational non-LTE spectrum in Fig. 1 (green curve) reproduces the general shape of measured signal (black curve) significantly better compared to that calculated with the rotational LTE assumption (turquoise curve). However, there are a number of small- and medium-size spectral features visible in the measured spectrum not present in the simulated one (green curve). So far the synthetic spectra discussed here were calculated ignoring line overlapping along the LOS.[3] In this study we employed our radiance model in both non-overlapping and overlapping mode. In the latter case the calculations treat spectral line overlapping of all bands (within a band and between lines of different bands) of all isotopes in the line-by-line (LBL) fashion (technical discussion is detailed in Rezac et al., 2015).

The effect of accounting for line overlapping is clearly demonstrated in spectrum plotted in red color. Two well-developed absorption features appeared, one around 2344 cm^{-1} and another one around 2324 cm^{-1}, which overlay well the corresponding features of measured spectrum. We found that the first of these features is caused by the absorption of radiation, which is emitted in the line R22e (here and below the line notations are taken from HITRAN) of the main isotope 10012–10002 SH band, by the nearly coincidental line R16e, which belongs to the fundamental band of isotope 628. The same is also true for the feature at 2324 cm^{-1}: here the emission line P4e of the 626 SH band 10012–10002 is blanketed by the line P15e of the first hot band 01111–01101 of the same isotope.

In addition, the "rotational non-LTE + overlapping on limb" spectrum (red curve) has an absorption feature around 2316 cm^{-1}, which is, however, much less pronounced than the one in the measured spectrum. The formation mechanism of this signature is rather complex. Here, the emission line, R9e, belonging to the 10011–10001 SH band of the 628 isotope (pumped by the 2.7 µm solar radiation), is attenuated by the two nearby lines Q31f and Q74f, from the 628 and 626 FH bands, respectively. To a smaller degree, several other lines located very closely to the R9e and belonging to various isotopic bands may also contribute to this absorption signature. It should be noted that none of the vibrational levels of bands whose lines are involved in the formation of this absorption feature were treated accounting for the rotational non-LTE in this study. In general, rotational non-LTE at the lower vibrational level can influence the band absorption, whereas at the upper level the band emission is impacted. To get a better agreement with the measured spectrum, regarding the said absorption feature, as well as in the region 2285–2305 cm^{-1}, where the synthetic spectrum does not reproduce a number of fine "wavy" features, we plan (a) to apply more detailed rotational non-LTE model and (b) to use the exact procedure of spectra convolution, such as the "zero padding", as applied to the PFS interferograms (Giuranna et al., 2005). This signal processing technique certainly contributes to the formation of these "wavy" features of measured spectra.

4 Conclusions

We present our first modeling results of the Mars Express PFS SWC daytime limb 4.3 µm spectra for the altitude region above 90 km. We show that the long-standing discrepancy between observed and calculated spectra in the cores and wings of the 4.3 µm region is explained by the non-thermal rotational distribution of the $^{12}C^{16}O_2$ molecules in upper vibrational levels 10011 and 10012 of the strong SH bands. The enhancement of the SH band wing emissions is caused (a) by intensive production of the CO_2 molecules in rotational states with $j > 30$ due to the absorption of solar radiation in optically thin wings of 2.7 µm bands and (b) by a short radiative lifetime of molecules in these states, which is insufficient at altitudes above 90 km for collisions to maintain rotation of excited molecules thermalized. As a result, redistribution of SH band intensities takes place going from band branch cores into their wings. This result confirms significant impact of rotational non-LTE on the CO_2 4.3 µm emissions of Martian and Venusian atmospheres, which was predicted by Kutepov et al. (1985) and Ogibalov and Kutepov (1989).

[3] We note here also that, although previous studies report using a forward model capable of treating line overlapping in limb calculations, its effects on PFS spectra were not discussed.

The PFS spectra provide the first strong evidence of this effect.

Although the rotational non-LTE on the levels 10011 and 10012 does an excellent job explaining the radiance redistribution observed in the measured spectra, more detailed simulations are still needed to investigate whether there are smaller-order effects caused by the rotational non-LTE at other CO_2 vibrational levels. However, accounting for rotational non-LTE significantly slows down the non-LTE calculations by an order of magnitude for the problem discussed in this paper.

Additional improvement in matching the 4.3 µm band shape/structure between simulated and PFS measured spectra was reached by accounting for spectral line overlapping (within each band and among lines of different bands) along the limb LOS. This allowed the reproduction of some fine absorption features in measured spectra that were missing in previous calculations, causing, however, a factor of 10 increase of the limb emission computing time. This additional computing time increase indicates the need for significant efforts aimed at optimizing the rotational non-LTE/line overlapping calculations to allow massive processing of measured PFS spectra.

The presented results are also important for diagnostics of other similar observations. For instance, the Venus Express VIRTIS spectra around 4.3 µm for tangent heights above 100–110 km, which are discussed in Gilli et al. (2009) and López-Valverde et al. (2011a), demonstrate remarkable resemblance of Mars Express PFS spectra analyzed in this study. Due to a well-known similarity of the CO_2 daytime emission formation mechanisms for both planets (Ogibalov and Kutepov, 1989) the Venus spectra obviously also require detailed rotational non-LTE/line overlapping analysis. These results may also be relevant for the analysis of limb mode measurements of the Trace Gas Orbiter/NOMAD instrument, which will start scientific operation in late 2017.

At last, we note that, as in previous studies, the following simplifications were applied in our simulations: (a) infinite-narrow field-of-view (FOV) approximation was used, and (b) detailed spectra convolution was not performed; only simple ($1\,cm^{-1}$)-triangle window (to match the instrument spectral resolution) averaging of monochromatic spectra calculated on a fine grid was applied. Neither of these, however, influence the main results of this study. Nevertheless, missing FOV averaging (in combination with insufficient matching of applied pressure/temperature model) may explain better agreement (see Fig. 1) between absolute emission values of an average spectrum measured for the tangent altitude of 115 km and the spectrum simulated for 120 km (compare black, red and orange lines in this figure). Additionally, simplified averaging of monochromatic spectra in combination with missing FOV averaging may cause certain fine structure inconsistencies between measured and simulated spectra compared in this study.

5 Data availability

The PFS data are available in the ESA Planetary Science Archive: ftp://psa.esac.esa.int/pub/mirror/MARS-EXPRESS/PFS/ (Giuranna, 2016). The results of calculations presented in Figs. 1 and 2 are available on the Open Science Framework website: doi:10.17605/OSF.IO/6S6UJ (Kutepov et al., 2017).

Acknowledgements. The authors cordially thank Marco Giuranna, the PI of PFS/MEX for providing us samples of PFS limb spectra with the emission features unexplained by the nominal non-LTE models, and for a very helpful discussion on the data quality and the general performance of the instrument. The work of AAK was supported by the NASA grant NNX08AL12G and the NSF grant AGS-1301762. The work of LR was partly supported by the DFG grant HA3261/7-1. The work of AGF was supported during his employment in the USA by the NASA grant NNX08AL12G and in France by the project "Towards a better interpretation of atmospheric phenomena" of the French National Program LEFE/INSU.

Edited by: M. Rapp
Reviewed by: two anonymous referees

References

Feofilov, A. G. and Kutepov, A. A.: Infrared Radiation in the Mesosphere and Lower Thermosphere: Energetic Effects and Remote Sensing, Surv. Geophys, 33, 1231–1280, doi:10.1007/s10712-012-9204-0, 2012.

Feofilov, A. G., Kutepov, A. A., Pesnell, W. D., Goldberg, R. A., Marshall, B. T., Gordley, L. L., García-Comas, M., López-Puertas, M., Manuilova, R. O., Yankovsky, V. A., Petelina, S. V., and Russell III, J. M.: Daytime SABER/TIMED observations of water vapor in the mesosphere: retrieval approach and first results, Atmos. Chem. Phys., 9, 8139–8158, doi:10.5194/acp-9-8139-2009, 2009.

Feofilov, A. G., Kutepov, A. A., Rezac, L., and Smith, M. D.: Extending MGS-TES temperature retrievals in the martian atmosphere up to 90 km: Retrieval approach and results, Icarus, 221, 949–959, 2012.

Formisano, V., Angrilli, F., Arnold, G., Atreya, S., Bianchini, G., Biondi, D., Blanco, A., Blecka, M. I., Coradini, A., Colangeli, L., Ekonomov, A., Esposito, F., Fonti, S., Giuranna, M., Grassi, D., Gnedykh, V., Grigoriev, A., Hansen, G., Hirsh, H., Khatuntsev, I., Kiselev, A., Ignatiev, N., Jurewicz, A., Lellouch, E., Lopez Moreno, J., Marten, A., Mattana, A., Maturilli, A., Mencarelli, E., Michalska, M., Moroz, V., Moshkin, B., Nespoli, F., Nikolsky, Y., Orfei, R., Orleanski, P., Orofino, V., Palomba, E., Patsaev, D., Piccioni, G., Rataj, M., Rodrigo, R., Rodriguez, J., Rossi, M., Saggin, B., Titov, D., and Zasova, L.: The Planetary Fourier Spectrometer (PFS) onboard the European Mars Express mission, Planet. Space Sci., 53, 963–974, doi:10.1016/j.pss.2004.12.006, 2005.

Formisano, V., Maturilli, A., Giuranna, M., D'Aversa, E., and López-Valverde, M.: Observations of non-LTE emission at 4–

5 microns with the planetary Fourier spectrometer abord the Mars Express mission, Icarus, 182, 51–67, 2006.

Gilli, G., López-Valverde, M. A., Drossart, P., Piccioni, G., Erard, S., and Cardesín Moinelo, A.: Limb observations of CO_2 and CO non-LTE emissions in the Venus atmosphere by VIRTIS/Venus Express, J. Geophys. Res.-Planet., 114, E00B29, doi:10.1029/2008JE003112, 2009.

Giuranna, M.: PFS Extended Mission 4 data, European Space Agency, available at: ftp://psa.esac.esa.int/pub/mirror/MARS-EXPRESS/PFS/, last access: 12 February 2016.

Giuranna, M., Formisano, V., Biondi, D., Ekonomov, A., Fonti, S., Grassi, D., Hirsch, H., Khatuntsev, I., Ignatiev, N., Michalska, M., Mattana, A., Maturilli, A., Moshkin, B. E., Mencarelli, E., Nespoli, F., Orfei, R., Orleanski, P., Piccioni, G., Rataj, M., Saggin, B., and Zasova, L.: Calibration of the Planetary Fourier Spectrometer short wavelength channel, Planet. Space Sci., 53, 975–991, doi:10.1016/j.pss.2004.12.007, 2005.

Gusev, O. A. and Kutepov, A. A.: Non-LTE Gas in Planetary Atmospheres, in: Stellar Atmosphere Modeling, edited by: Hubeny, I., Mihalas, D., and Werner, K., vol. 288, Astronomical Society of the Pacific Conference Series, San Francisco, USA, 318–330, 2003.

Gusev, O. A., Kaufmann, M., Grossmann, K., Schmidlin, F., and Shepherd, M.: Atmospheric neutral temperature distribution at the mesopause altitude, J. Atmos. Sol.-Terr. Phy., 68, 1684–1697, 2006.

Hartmann, J. M., Boulet, C., and Robert, D.: Collisional Effects on Molecular Spectra, Elsevier, Amsterdam, the Netherlands, 2008.

Hartogh, P., Medvedev, A. S., Kuroda, T., Saito, R., Villanueva, G., Feofilov, A. G., Kutepov, A. A., and Berger, U.: Description and climatology of a new general circulation model of the Martian atmosphere, J. Geophys. Res.-Planet., 110, E11008, doi:10.1029/2005JE002498, 2005.

Hubeny, I. and Lanz, T.: Model Photospheres with Accelerated Lambda Iteration, in: Stellar Atmosphere Modeling, edited by: Hubeny, I., Mihalas, D., and Werner, K., vol. 288, Astronomical Society of the Pacific Conference Series, San Francisco, USA, 51–68, 2003.

Kaufmann, M., Gusev, O. A., Grossmann, K. U., Roble, R. G., Hagan, M. E., Hartsough, C., and Kutepov, A. A.: The vertical and horizontal distribution of CO_2 densities in the upper mesosphere and lower thermosphere as measured by CRISTA, J. Geophys. Res., 107, 8182, doi:10.1029/2001JD000704, 2002.

Kaufmann, M., Gusev, O. A., Grossmann, K. U., Martín-Torres, F. J., Marsh, D. R., and Kutepov, A. A.: Satellite observations of daytime and nighttime ozone in the mesosphere and lower thermosphere, J. Geophys. Res.-Atmos., 108, 4272, doi:10.1029/2002JD002800, 2003.

Kutepov, A. A., Hummer, D. G., and Moore, C. B.: Rotational relaxation of the 00^01 level of CO_2 including radiative transfer in the 4.3 µm band of planetary atmospheres, J. Quant. Spectrosc. Ra., 34, 101–114, 1985.

Kutepov, A. A., Kunze, D., Hummer, D. G., and Rybicki, G. B.: The solution of radiative transfer problems in molecular bands without the LTE assumption by accelerated lambda iteration methods, J. Quant. Spectrosc. Ra., 46, 347–365, doi:10.1016/0022-4073(91)90038-R, 1991.

Kutepov, A. A., Oelhaf, H., and Fischer, H.: Non-LTE radiative transfer in the 4.7 and 2.3 µm bands of CO: vibration-rotational non-LTE and its effects on limb radiance, J. Quant. Spectrosc. Ra., 57, 317–339, doi:10.1016/S0022-4073(96)00142-2, 1997.

Kutepov, A. A., Gusev, O. A., and Ogibalov, V. P.: Solution of the Non-LTE Problem for Molecular Gas in Planetary Atmospheres: Superiority of Accelerated Lambda Iteration, J. Quant. Spectrosc. Ra., 60, 199–220, 1998.

Kutepov, A. A., Feofilov, A. G., Marshall, B. T., Gordley, L. L., Pesnell, W. D., Goldberg, R. A., and Russell, J. M.: SABER temperature observations in the summer polar mesosphere and lower thermosphere: Importance of accounting for the CO_2 ν_2 quanta V-V exchange, Geophys. Res. Lett., 33, L21809, doi:10.1029/2006GL026591, 2006.

Kutepov, A. A., Feofilov, A. G., Medvedev, A. S., Pauldrach, A. W. A., and Hartogh, P.: Small-scale temperature fluctuations associated with gravity waves cause additional radiative cooling of mesopause the region, Geophys. Res. Lett., 34, L24807, doi:10.1029/2007GL032392, 2007.

Kutepov, A. A., Rezac, L., and Feofilov, A. G.: Rotational non-LTE effect in the 4.3 µm PFS-MEX limb spectra, Physics Department, The Catholic University of America, Washington, D.C., USA, doi:10.17605/OSF.IO/6S6UJ, 2017.

López-Valverde, M., López-Puertas, M., López-Moreno, J. J., Formisano, V., Grassi, D., Maturilli, A., Lellouch, E., and Drossart, P.: Analysis of CO_2 non-LTE emissions at 4.3 µm in the Martian atmosphere as observed by PFS/Mars Express and SWS/ISO, Planet. Space Sci., 53, 1079–1087, 2005.

López-Valverde, M. A., López-Puertas, M., Funke, B., Gilli, G., Garcia-Comas, M., Drossart, P., Piccioni, G., and Formisano, V.: Modeling the atmospheric limb emission of CO $_2$ at 4.3 µm in the terrestrial planets, Planet. Space Sci., 59, 988–998, doi:10.1016/j.pss.2010.02.001, 2011a.

López-Valverde, M. A., Sonnabend, G., Sornig, M., and Kroetz, P.: Modelling the atmospheric CO_2 10 µm non-thermal emission in Mars and Venus at high spectral resolution, Planet. Space Sci., 59, 99–1009, doi:10.1016/j.pss.2010.11.011, 2011b.

Maguire, W. C., Pearl, J. C., Smith, M. D., Conrath, J., Kutepov, A. A., Kaelberer, M. S., Winter, E., and Christensen, P. R.: Observations of high-altitude CO_2 hot bands in Mars by the orbiting Thermal Emission Spectrometer, Geophys. Res. Lett., 127, 5063, doi:10.1029/2001JE001516, 2002.

Ogibalov, V. P. and Kutepov, A. A.: An approximate solution for radiative transfer in the 4.3 µm CO_2 band: thick atmosphere with breakdown of rotational LTE, Sov. Astron., 33, 511–519, 1989.

Pack, R. T.: Pressure broadening of the dipole and Raman lines of CO_2 by He and Ar. Temperature dependence, J. Chem. Phys., 70, 3424–3433, doi:10.1063/1.437876, 1979.

Pauldrach, A. W. A.: Hot Stars: Old-Fashioned or Trendy? (with 24 Figures), in: Reviews in Modern Astronomy, edited by: Schielicke, R. E., Wiley, New York, USA, vol. 16, 141–177, 2003.

Pauldrach, A. W. A., Kudritzki, R. P., Puls, J., Butler, K., and Hunsinger, J.: Radiation-driven winds of hot luminous stars. 12: A first step towards detailed UV-line diagnostics of O-stars, Astron. Astrophys., 283, 525–560, 1994.

Pauldrach, A. W. A., Hoffmann, T. L., and Lennon, M.: Radiation-driven winds of hot luminous stars. XIII. A description of NLTE line blocking and blanketing towards realistic models for expanding atmospheres, Astron. Astrophys., 375, 161–195, doi:10.1051/0004-6361:20010805, 2001.

Preston, R. K. and Pack, R. T.: Classical trajectory studies of rotational transitions in Ar-CO_2 collisions, J. Chem. Phys., 66, 2480–2487, 1977.

Rezac, L., Kutepov, A., Russell, J. M., Feofilov, A. G., Yue, J., and Goldberg, R. A.: Simultaneous retrieval of T(p) and CO_2 VMR from two-channel non-LTE limb radiances and application to daytime SABER/TIMED measurements, J. Atmos. Sol.-Terr. Phy., 130, 23–42, doi:10.1016/j.jastp.2015.05.004, 2015.

Rothman, L., Gordon, I., Babikov, Y., Barbe, A., Benner, D. C., Bernath, P., Birk, M., Bizzocchi, L., Boudon, V., Brown, L., Campargue, A., Chance, K., Cohen, E., Coudert, L., Devi, V., Drouin, B., Fayt, A., Flaud, J.-M., Gamache, R., Harrison, J., Hartmann, J.-M., Hill, C., Hodges, J., Jacquemart, D., Jolly, A., Lamouroux, J., Roy, R. L., Li, G., Long, D., Lyulin, O., Mackie, C., Massie, S., Mikhailenko, S., Muller, H., Naumenko, O., Nikitin, A., Orphal, J., Perevalov, V., Perrin, A., Polovtseva, E., Richard, C., Smith, M., Starikova, E., Sung, K., Tashkun, S., Tennyson, J., Toon, G., Tyuterev, V., and Wagner, G.: The {HITRAN2012} molecular spectroscopic database, J. Quant. Spectrosc. Ra., 130, 4–50, 2013.

Rybicki, G. B. and Hummer, D. G.: An accelerated lambda iteration method for multilevel radiative transfer I. Non-overlapping lines with background continuum, Astron. Astrophys., 245, 171–181, 1991.

Shved, G. M., Kutepov, A. A., and Ogibalov, V. P.: Non-local thermodynamic equilibrium in CO_2 in the middle atmosphere. I. Input data and populations of the ν_3 mode manifold states, J. Atmos. Sol.-Terr. Phy., 60, 289–314, 1998.

Werner, K.: Construction of non-LTE model atmospheres using approximate lambda operators, Astron. Astrophys., 161, 177–182, 1986.

Werner, K.: Stellar Atmospheres in Non-LTE: Model Construction and Line Formation Calculations using Approximate Lambda Operators, in: Numerical Radiative Transfer, edited by: Kalkofen, K., University Press, Cambridge, UK, 67–117, 1978.